HHS Public Access

Author manuscript

Mol Cell Biochem. Author manuscript; available in PMC 2024 August 05.

Published in final edited form as:

Mol Cell Biochem. 2023 April ; 478(4): 939–948. doi:10.1007/s11010-022-04555-5.

Twist alters the breast tumor microenvironment via choline kinase to facilitate an aggressive phenotype

Farhad Vesuna[1], **Marie-France Penet**[1,2], **Noriko Mori**[1], **Zaver M. Bhujwalla**[1,2,3], **Venu Raman**[1,2,4,5]

[1]Division of Cancer Imaging Research, Department of Radiology, Johns Hopkins University School of Medicine, Baltimore, MD, USA

[2]Department of Oncology, Johns Hopkins University School of Medicine, Baltimore, MD, USA

[3]Department of Radiation Oncology and Molecular Radiation Sciences, Johns Hopkins University School of Medicine, Baltimore, MD, USA

[4]Department of Pathology, University Medical Center Utrecht, Utrecht, The Netherlands

[5]Department of Pharmacology, Johns Hopkins University School of Medicine, Baltimore, MD, USA

Abstract

Twist (TWIST1) is a gene required for cell fate specification in embryos and its expression in mammary epithelium can initiate tumorigenesis through the epithelial-mesenchymal transition. To identify downstream target genes of Twist in breast cancer, we performed microarray analysis on the transgenic breast cancer cell line, MCF-7/Twist. One of the targets identified was choline kinase whose upregulation resulted in increased cellular phosphocholine and total choline containing compounds—a characteristic observed in highly aggressive metastatic cancers. To study the interactions between Twist, choline kinase, and their effect on the microenvironment, we used ^{1}H magnetic resonance spectroscopy and found significantly higher phosphocholine and total choline, as well as increased phosphocholine/glycerophosphocholine ratio in MCF-7/Twist cells. We also observed significant increases in extracellular glucose, lactate, and [H +] ion concentrations in the MCF-7/Twist cells. Magnetic resonance imaging of MCF-7/Twist orthotopic breast tumors showed a significant increase in vascular volume and permeability surface area product compared to control tumors. In addition, by reverse transcription—quantitative polymerase chain reaction, we discovered that Twist upregulated choline kinase expression in estrogen receptor negative breast cancer cell lines through FOXA1 downregulation. Moreover, using The Cancer Genome Atlas database, we observed a significant inverse relationship between FOXA1 and choline kinase expression and propose that it could act as a modulator of the Twist/choline kinase axis. The data presented indicate that Twist is a driver of choline kinase expression in breast cancer cells via FOXA1 resulting in the generation of an aggressive breast cancer phenotype.

✉Venu Raman, vraman2@jhmi.edu.

Conflict of interest The author reports no conflicts of interest in this work.

Keywords

Metastasis; Breast cancer; Magnetic resonance spectroscopy; Cellular signaling; Vascular volume; Vascular permeability

Introduction

Twist is a basic helix-loop-helix (bHLH) transcription factor that exerts its function through dimer formation [1, 2] and is essential in cell fate specification, tissue differentiation, and growth regulation [3–13] during development. Mutations in the *Twist* gene can also give rise to Saethre-Chotzen syndrome, an autosomal dominant disease, which results in craniosynostosis [14, 15]. In addition, mutations in the helix domain of the *Twist* gene can cause subcellular mislocalization and increased degradation of its protein product resulting in the repression of pro-inflammatory cytokine gene expression [16, 17]. Evidence from our laboratory and others indicates that Twist is involved in several pathways that lead to the formation of cancer by halting differentiation, controlling apoptosis [18], interfering with the p53 tumor suppressor pathway [19], and inducing an epithelial-mesenchymal transition (EMT) [20, 21]. In addition, increased expression of Twist in nasopharyngeal, bladder, ovarian, and prostate tumor cell lines is associated with resistance to Taxol and other drugs that disrupt microtubules [22]. Twist can also bind to p300 and decrease its histone acetyl-transferase activity [23]. In breast cancers, we have shown that Twist binds to HOXA5 [18], upregulates VEGF [20] and miR-22 [24], promotes chromosomal instability [25], and represses E-cadherin [26], CD24 [27], and ERα [28] expression.

To identify downstream target genes of Twist, we performed microarray analysis of the transgenic breast cancer cell line, MCF-7/Twist [20, 29]. One of the targets identified was choline kinase (CHKA). Numerous studies have demonstrated the dysregulation of phosphocholine (PC) and glycerophosphocholine (GPC), two key molecules linked to choline metabolism, in advanced breast cancer [30–32]. Upregulation of choline kinase levels in cancer cells results in increased cellular PC and total choline containing compounds —a characteristic observed in highly aggressive metastatic cancers. We hypothesized that the regulation of choline kinase levels, either directly or indirectly through Twist, could play a role in detection and treatment of breast cancer.

We used high-resolution ^{1}H magnetic resonance spectroscopy (MRS) to show that MCF-7/Twist cells have significantly increased choline kinase activity as indicated by increased phosphocholine levels. Microarray analysis of MCF-7/Twist cells identified increased expression of lactate dehydrogenase that may have influenced the extracellular pH of the tumor microenvironment. We found increased levels of glucose, lactate, and hydrogen ions in the expended media of MCF-7/Twist cells. In addition, we used magnetic resonance imaging (MRI) of MCF-7/Twist xenograft tumors to demonstrate an increase in vascular volume and permeability surface area product. Mechanistically, expression levels of FOXA1 and CDK8 were inversely correlated with Twist expression in ER-negative cell lines. From TCGA analysis, we showed that FOXA1 inversely correlates with CHKA and CHKB expression in breast cancers and that Twist could drive CHKA and CHKB expression via the

downregulation of FOXA1 and CDK8. Based on these observations, we conclude that Twist promotes an aggressive phenotype by altering cellular physiology of the breast epithelium by modulating CHK expression through FOXA1 and CDK8, thus promoting breast cancer invasion and metastasis.

Materials and methods

Cell lines

MCF-7 cells were obtained from ATCC (Manassas, VA) and periodically tested for mycoplasma contamination. MCF-7/Twist cells were developed in our laboratory [20, 29].

Immunoblotting

Immunoblotting was performed on proteins extracted in 2% SDS from cell pellets and run on 10–12% SDS-PAGE. Detection was performed using a chemiluminescent system. Antibodies to Twist were developed in our laboratory [20] while choline kinase alpha (custom-made by Proteintech Group, Inc., Chicago, IL) and Actin antibodies (Millipore Sigma, Darmstadt, Germany) were obtained commercially.

Dual-phase cell extraction and ^{1}H MRS

Water-soluble as well as lipid extracts were obtained from more than 2×10^7 cells using a dual-phase extraction method [31] with the water-soluble phase used for the ^{1}H MRS. Briefly, cells were harvested by trypsinization, and counted for quantitation. The pelleted cells were mixed with 4 ml of ice-cold methanol and vigorously vortexed. After keeping samples on ice for 15 min, 4 ml of chloroform was added, vortexed vigorously and kept on ice for 10 min. Finally, 4 ml of water was added and mixed well. All operations were performed on ice and samples were stored at 4 °C overnight for phase separation and later centrifuged at 15,000 g at 4 °C for 30 min. The water/methanol phase containing water-soluble metabolites such as choline (Cho), PC, and GPC was treated with ~ 100 mg of chelex beads (Sigma-Aldrich, St. Louis, MO) to remove any divalent cations. After removing the beads, methanol was evaporated using a rotary evaporator. The remaining water phase was lyophilized and stored at −20 °C until use. Water-soluble extracts from cells were resuspended in 0.6 ml of deuterated water (D_2O) containing 2.4×10^{-7} mol of 3-(trimethylsilyl)propionic 2,2,3,3-d_4 acid (TSP; Sigma-Aldrich, St. Louis, MO) as an internal standard for MR spectral analysis. Fully relaxed ^{1}H MR spectra of the water-soluble extracts were acquired on a Bruker Avance 11.7 T spectrometer (Bruker BioSpin Corp., Billerica, MA) with flip angle = 30°, sweep width = 10,000 Hz, repetition time = 11.2 s, block size = 32 K, and scans = 128. MR spectra were analyzed using Bruker XWIN-NMR 3.5 software (Bruker BioSpin). Signal integrals of N-$(CH_3)_3$ of Cho, PC, and GPC from within the 3.20–3.24 ppm region were determined, normalized to cell numbers, and compared to the standard (TSP) to obtain relative concentrations in arbitrary units (A.U.).

Glucose, lactate, and pHe measurements

MCF-7 and MCF-7/Twist cells were grown in MEM supplemented with 10% FCS at an initial plating density of 15,000 cells/well of a 24-well plate. The following day, 250 μl of media was withdrawn from two wells and estimated for lactate and pH levels on an ABL

700 blood gas analyzer (Radiometer America Inc., Westlake, OH). The number of cells in each well were subsequently counted. Glucose and lactate were measured as mMol/l units and normalized to cell counts. pH was converted to the moles of [H +] by the formula [H +] = $10^{(-pH)}$ and normalized to cell counts.

MR acquisitions

All imaging studies were performed on a 9.4 T Bruker spectrometer (Bruker, Billerica, MA) using a home-built solenoid coil placed around the tumors. Mice were anesthetized with an intraperitoneal injection of ketamine (25 mg/kg; Phoenix Scientific, Inc., St Joseph, MO) and acepromazine (2.5 mg/kg; Aveco, Phoenix Scientific).

Vascular imaging

The tail vein was catheterized before placing the animal in the spectrometer. Vascular imaging was performed as previously described [33]. Briefly, multislice relaxation rate ($1/T_1$) maps were obtained by a saturation recovery method combined with fast T_1 SNAPSHOT-FLASH imaging (flip angle of 10°, echo time of 2 ms). First, an Mo map with a recovery delay of 10 s was acquired following which images of four slices (1 mm thick), acquired with an in-plane spatial resolution of 125 μm (128 × 128 matrix, 16 mm field of view (FOV), 8 averages), were obtained for three relaxation delays (100 ms, 500 ms, and 1 s). These T_1 recovery maps were obtained before i.v. injection of 0.2 ml of 60 mg/ml albumin-GdDTPA in saline (dose of 500 mg/kg) and repeated over a 21-min period, starting 3 min after i.v. injection of the contrast agent. Albumin-GdDTPA was synthesized based on the method of Ogan [34]. At the end of the imaging studies, the T_1 of the blood was measured. Relaxation maps were reconstructed from data sets for the three different relaxation times and the Mo dataset on a pixel-by-pixel basis. Vascular volume and permeability surface area product (PSP) maps were generated from the ratio of ($1/T_1$) values in the images to that of blood. The slope of ($1/T_1$) ratios versus time in each pixel was used to compute PSP, and the intercept of the line at zero time was used to compute vascular volume. Data were processed with an operator-independent computer program that enabled selection, mapping, and display of the regions with a routine written using Interactive Data Language (IDL, Research Systems, Boulder, CO). For both vascular volume and PSP, we analyzed the averages of the highest 10%, 25% and 100% of the non-zero values and also derived the total averages over the entire tumor.

Metabolic imaging

Metabolic maps of total choline (tCho) were obtained from a 4 mm thick slice using a 2D chemical shift imaging (CSI) sequence with VAPOR water suppression [35]. A reference image from a 4 mm thick central tumor slice was acquired using a spin-echo sequence (msme-tomo, Bruker). Water-suppressed MRSI was performed on the same central slice, with an in-plane resolution of 1 × 1 mm per pixel using a 2D CSI sequence with VAPOR water suppression and the following variables: echo time (TE) of 272 ms, repetition time of 1000 ms, FOV of 1.6 × 1.6 cm, 256 phase encode steps (16 × 16 voxels), number of scans (NS) of 8, block size of 1024, and sweep width of 7000 Hz. Reference 2D CSI images of the unsuppressed water signal were acquired of the same slice with TE = 20 ms and NS

= 2, with all other variables remaining the same. Quantitative maps in arbitrary units were generated according to the method described by Bolan et al. [36].

RT-qPCR

Total RNA was extracted from cell lines using an RNA extraction kit (Qiagen, Germantown, MD) and converted to cDNA (Bio-Rad, Hercules, CA). cDNA was amplified in a Bio-Rad CFX Touch instrument by quantitative PCR using gene-specific primers for CHK, FOXA1, and CDK8. Data were plotted using ddCt values normalized to the housekeeper gene 36B4.

TCGA and ENCODE data analysis

Breast invasive carcinoma data were analyzed from the TCGA PanCancer Atlas which had a sample size of 1,084 patients. mRNA expression correlations were extracted from the database using cBioPortal [37, 38] which utilizes RSEM [39] and are batch normalized from Illumina HiSeq RNASeqV2 platform. ENCODE data to show binding of transcription factors to gene promoters were performed using Harmonizome [40].

Results

Twist upregulates choline kinase expression in MCF-7 cells

Overexpression of choline kinase and its effects on choline metabolism (PC and GPC) have been demonstrated as useful markers in identifying invasive phenotypes [32]. Based on the genotypic alterations observed in MCF-7/Twist cells, we analyzed microarray data for the expression of choline kinase in MCF-7/Twist cells. We observed a two-fold increase in choline kinase mRNA levels in MCF-7/Twist cells when compared to parental MCF-7 cells. Subsequent analysis by immunoblotting demonstrated that choline kinase protein levels were six-fold more in MCF-7/Twist than in MCF-7 cells (Fig. 1A). In addition, MCF-7/Twist cells showed a significant increase in PC levels, an indicator of choline kinase activity, when analyzed by high-resolution ^{1}H MRS (Fig. 1B). Significant increases in phosphocholine (from 5.3 to 30.3 A.U.), total choline (from 13.9 to 36.4 A.U.), and PC/GPC ratio (0.7–5.7 A.U.) were observed (Fig. 1C). Overall, the results indicated that the overexpression of Twist increased choline kinase levels and its effector functions.

Increased efflux of Lactate and H + in Twist overexpressing cells

Initial microarray analysis provided strong evidence of upregulated lactate dehydrogenase levels in MCF-7/Twist cells (over 7000-fold) compared to parental MCF-7 cells. To verify if this corresponded to increased glucose, lactate, and hydrogen ions [H^+] levels, we measured extracellular glucose, lactate, and hydrogen ions [H^+] in MCF-7 and MCF-7/Twist media over a period of four days. As seen in Fig. 2A, there was significantly higher extracellular glucose in MCF-7/Twist cells compared to MCF-7 cells by 2.7-fold on day one, 9.6-fold on day two, 246-fold on day three, and 143-fold on day four (Fig. 2A). Lactate levels were higher in MCF-7/Twist cells by 2.1-fold on day one, fourfold on day two, and 4.5-fold on days three and four (Fig. 2B). There was also a significant increase in extracellular [H^+] ions in MCF-7/Twist media as compared to MCF-7. [H^+] ions increased 2.4-fold on day one, 5.2-fold on day two, 4.9-fold on day three, and 4.5-fold on day four (Fig. 2C).

Overexpression of Twist causes an increase in VV and PS in MCF-7 orthotopic tumors

To determine the biochemical and physiological alterations caused by Twist in orthotopic breast tumors, we initiated MCF-7/Twist and MCF-7 cell tumors in female SCID mice using 1×10^6 cells per inoculation in the second thoracic mammary fat pad. We scanned the MCF-7 ($n = 5$) and MCF-7/Twist ($n = 5$) tumors when they reached a size of approximately 600 mm^3 (Fig. 3A). We observed higher vascular volume (VV) and permeability surface area (PS) in the MCF-7/Twist tumors compared to the MCF-7 tumors as seen from the representative vascular volume and permeability surface area product maps (Fig. 3B). This was confirmed after analyzing all the tumor data, which demonstrated a significant increase in both VV and PS in MCF-7/Twist tumors (Fig. 3C–D). VV increased 1.7-fold at 10–25%, 2.4-fold at 100%, and the total VV increased 3.5-fold (Fig. 3C). PS increased 3.2-fold at 10%, 2.9-fold at 25%, 2.5-fold at 100%, and total PS increased 2.9-fold (Fig. 3D).

Twist orthotopic tumors tend to have lower total choline

To study the effect of Twist on tCho levels in vivo in orthotopic breast tumors, we acquired metabolic maps of tCho on a 4 mm thick slice. Representative tCho maps of MCF-7 and MCF-7/Twist are shown in Fig. 4A. As seen in Fig. 4B, the metabolic data showed that the aggressive MCF-7/Twist tumors had lower choline than the control MCF-7 cells in the cohort of animals scanned (MCF-7, $n = 7$; MCF-7/Twist, $n = 14$). However, this was not significant. This decrease in total choline could be due to necrosis observed in the MCF-7/Twist tumors which is visible as a lack of signal in the central portion of the tumors. This could be due to their faster growth rate compared to the MCF-7 tumors.

Twist regulation of choline kinase may be modulated by FOXA1 and CDK8

To investigate the mechanisms of Twist regulation of CHKA, we studied the expression levels of FOXA1 and CDK8 by RT-qPCR in various breast cell lines using MCF-7 as a baseline for expression. We have earlier demonstrated that Twist downregulates ERα expression in breast cancers [28]. From ENCODE data, it was evident that the FOXA1 transcription factor binds to CHKA and CHKB promoters. Also, there is ENCODE data to indicate that FOXA1 binds to CDK8 which binds to CHKB. Based on this regulatory axis of FOXA1/CDK8/CHK, we hypothesized that Twist could be a driver controlling expression of CHKA and CHKB expression via FOXA1 and CDK8. As seen in Fig. 5, the normal cell lines MCF 12A and MCF 10A had negligible expression of CHK, FOXA1, and CDK8. CHK expression ($\log_2$ FC = −2.1, −2.9) correlated directly with FOXA1 expression ($\log_2$ FC = −6.0, −9.3) and CDK8 ($\log_2$ FC = −1.0, −1.7) in these cell lines. Both the ER + cell lines T-47D and MCF-7 showed very low expression of CHK ($\log_2$ FC = 0.5, 0). The ER- cell lines displayed positive and negative correlations between expression of CHK, FOXA1, and CDK8 expression depending upon the cell line. The MCF-7/Twist cell line displayed a similar pattern towards an inverse relationship between CHK ($\log_2$ FC = 2.9) and FOXA1 ($\log_2$ FC = 0.3) and a direct correlation with CDK8 expression ($\log_2$ FC = 2.4). MDA-MB-241 showed an inverse correlation between CHK expression ($\log_2$ FC = 2.4), FOXA1 expression ($\log_2$ FC = −8.1), and CDK8 expression ($\log_2$ FC = −0.5). The SUM 149PT cell line displayed a negative correlation between CHK expression ($\log_2$ FC = 2.5) and FOXA1 expression ($\log_2$ FC = −3.4), and a positive correlation with CDK8 expression

(log_2 FC = 2.5). Overall, there was a direct correlation between CHK and FOXA1 in ER + cell lines and an inverse correlation in ER- cell lines.

Twist, FOXA1, and CDK8 expression in breast cancer and correlation with CHKA and CHKB

From TCGA data for 1,084 breast cancer patients, we extracted correlations between mRNA expression patterns of Twist, FOXA1, ESR1, CDK8, CHKA, and CHKB expression. There was a significant inverse relationship between FOXA1 and CHKA (Fig. 6A), FOXA1 and CHKB (Fig. 6B), and FOXA1 and CDK8 expression (Fig. 6C). There was also an inverse correlation between CDK8 and CHKB expression (Fig. 6D) as well as an inverse relationship between Twist and FOXA1 expression (Fig. 6E), while there was a direct correlation between FOXA1 and ESR1 expression (Fig. 6F). Overall, we hypothesize that Twist expression drives CHKA (immunoblotting), CHKB (microarray data), and downregulates FOXA1 (RT-qPCR). This downregulation of FOXA1 in turn directly upregulates CHKA and CHKB and indirectly via CDK8 (Fig. 7).

Discussion

In recent years, there have been considerable advancements into the role of the tumor microenvironment in breast cancer development and progression [41]. There is significant interest as to how molecular alterations to the tumor microenvironment contribute to therapeutic efficacy, drug resistance, as well as predict clinical outcome [42]. To understand the tumor microenvironment, numerous models have been developed such as 2D and 3D in vitro models to understand cell–cell and cell-extracellular matrix interactions [41]. These models have provided us with a better understanding of specific tumor microenvironment changes that facilitate malignant progression and potentially identify new specific microenvironment derived molecules as prognostic markers or drug targets [43, 44]. In our ongoing interest to decipher the role of Twist in breast cancer biogenesis, we have already demonstrated the functional role of Twist in EMT and angiogenesis [20], p53 response to γ-radiation [18], and regulation of E-cadherin [26] and ER [28]. In support of our findings, there are reports indicating that Twist expression is required for embryonic vascular development in Xenopus [45]. Also, recent evidence indicates that Twist expression promotes recruitment of stromal macrophages via CCL2 induction to promote angiogenesis and tumor progression [46]. In addition, it has been shown that Twist promotes angiogenesis in pancreatic cancer through the regulation of miR-497/VEGFA axis [47].

Continuing investigation of the role of Twist in breast cancer biogenesis led us to identity choline kinase as a target of Twist in breast cancer cells. Choline metabolism has been associated with an aggressive cancer phenotype and this could be linked to cells undergoing EMT. Observations that Twist expression facilitates EMT [20], and that choline kinase levels are upregulated in Twist overexpressing cells suggest that Twist regulates multiple signaling pathways in breast cancer cells to facilitate an aggressive phenotype. Interestingly, choline kinase inhibition has been shown to induce tumor regression, decrease metastasis, and increase drug sensitivity [48, 49].

Our data indicates that Twist expression directly correlates with choline kinase expression in breast cancer cells and regulates it. We observed an increase in CHKA by immunoblotting and demonstrated a functional increase in total choline and increase in PC/GPC ratio by high-resolution MRS of MCF-7/Twist cells. HIF-1α is the other major transcription factor that directly regulates choline kinase expression in breast cancer [50]. MCF-7/Twist cells showed increased extracellular glucose, lactate, and hydrogen ions [H^+] that could alter proteolytic activity and remodel the extracellular matrix. This could possibly be occurring through increased expression of HIF-1α which regulates glucose lactate dehydrogenase expression and glucose metabolism [51] and is also shown to regulate Twist [52]. Also, aggressive cancers have been shown to utilize aerobic glycolysis resulting in the export of H^+ equivalents from the cytoplasm [53]. Such activities raise the intracellular pH (pHi) and acidify the extracellular pH (PHe). This dynamic fluidity of maintaining an alkaline pHi promotes increased glycolytic flux, which is characteristic of aggressive cancers [53]. We showed that MCF-7/Twist tumors had a higher vascular volume and permeability surface area product which could result in remodeling of the extracellular matrix. This could cause increased angiogenesis, thus promoting tumor growth. This is consistent with our earlier results which indicated that Twist promotes in vivo angiogenesis via regulation VEGF [20]. Interestingly, we observed a significant drop in total choline in MCF-7/Twist tumors which was opposite to our in vitro results. This could possibly be due to necrosis observed in the central regions of the rapidly growing MCF-7/Twist tumors (Figs. 3B, 4A). RT-qPCR results showed an inverse relationship between Twist and FOXA1 and CDK8 only in ER-negative cell lines. This is in line with earlier data that show a relationship between FOXA1 and GATA-3 in ER-negative breast tumors [54]. This supports our hypothesis that Twist regulates FOXA1 which in turn regulates CHKA and CHKB. Interestingly, there is evidence to indicate that Twist directly represses the transcriptional activity of FOXA1 in breast cancer cells [55]. To study whether our hypotheses held up in breast tumors, we used publicly available TCGA data from 1084 breast cancer patients that had expression values for these genes. We confirmed that Twist and FOXA1 were inversely correlated in expression and so were FOXA1 and CHKA/CHKB. These results provide evidence that expression of Twist alters both intracellular and extracellular parameters to enhance tumor growth and facilitate metastasis by modifying the tumor microenvironment brought about by regulating choline kinase expression through FOXA1. In summary, we found that Twist expression downregulates FOXA1 resulting in decrease CHKA and CHKB expression. Thus the Twist/FOXA1/CHKA axis could be responsible for mediating enhanced migration, invasion, and metastasis of breast cancer cells. This, in combination with the acidification of the extracellular environment, facilitates a permissive environment which provides an advantage for cancer cells. However, there needs to more investigation to determine if the combinatorial effect of the Twist/FOXA1/CHKA axis to promote aggressive breast cancers is linear and is a dominant contributing effector metastasis.

Acknowledgements

We acknowledge help from Ksenija Grgac. Some of the results shown here are in whole or part based upon data generated by the TCGA Research Network: https://www.cancer.gov/tcga.

Funding

Funding was provided by the NIH through grants R01CA082337 to MFP, NM, and ZMB and R01CA097226 to VR.

Data availability

The datasets analyzed during the current study are available in the Gene Expression Omnibus (GEO) repository under series GSE87705 (http://www.ncbi.nlm.nih.gov/geo/query/acc.cgi?acc=GSE87705).

Abbreviations

FOV	Field of view
MRI	Magnetic resonance imaging
VV	Vascular volume
PS	Permeability surface area product
MRS	Magnetic resonance spectroscopy
PC	Phosphocholine
GPC	Glycerophosphocholine
tCho	Total choline
RT-qPCR	Reverse transcription quantitative polymerase chain reaction
TCGA	The Cancer Gene Atlas

References

1. Rose CS, Malcolm S (1997) A TWIST in development. Trends Genet 13(10):384–387 [PubMed: 9351337]
2. Bourgeois P, Stoetzel C, Bolcato-Bellemin AL, Mattei MG, Perrin-Schmitt F (1996) The human H-twist gene is located at 7p21 and encodes a B-HLH protein that is 96% similar to its murine M-twist counterpart. Mamm Genome 7(12):915–917 [PubMed: 8995765]
3. Gitelman I (1997) Twist protein in mouse embryogenesis. Dev Biol 189(2):205–214 [PubMed: 9299114]
4. Technau U, Scholz CB (2003) Origin and evolution of endoderm and mesoderm. Int J Dev Biol 47(7–8):531–539 [PubMed: 14756329]
5. Castanon I, Von Stetina S, Kass J, Baylies MK (2001) Dimerization partners determine the activity of the Twist bHLH protein during Drosophila mesoderm development. Development 128(16):3145–3159 [PubMed: 11688563]
6. Cripps RM, Black BL, Zhao B, Lien CL, Schulz RA, Olson EN (1998) The myogenic regulatory gene Mef2 is a direct target for transcriptional activation by twist during Drosophila myogenesis. Genes Dev 12(3):422–434 [PubMed: 9450935]
7. Hamamori Y, Wu HY, Sartorelli V, Kedes L (1997) The basic domain of myogenic basic helix-loop-helix (bHLH) proteins is the novel target for direct inhibition by another bHLH protein. Twist Mol Cell Biol 17(11):6563–6573 [PubMed: 9343420]
8. Hebrok M, Fuchtbauer A, Fuchtbauer EM (1997) Repression of muscle-specific gene activation by the murine Twist protein. Exp Cell Res 232(2):295–303 [PubMed: 9168805]

9. Lee MS, Lowe GN, Strong DD, Wergedal JE, Glackin CA (1999) TWIST, a basic helix-loop-helix transcription factor, can regulate the human osteogenic lineage. J Cell Biochem 75(4):566–577 [PubMed: 10572240]
10. Li L, Cserjesi P, Olson EN (1995) Dermo-1: a novel twist-related bHLH protein expressed in the developing dermis. Dev Biol 172(1):280–292 [PubMed: 7589808]
11. Spicer DB, Rhee J, Cheung WL, Lassar AB (1996) Inhibition of myogenic bHLH and MEF2 transcription factors by the bHLH protein Twist. Science 272(5267):1476–1480 [PubMed: 8633239]
12. Verzi MP, Anderson JP, Dodou E et al. (2002) N-twist, an evolutionarily conserved bHLH protein expressed in the developing CNS, functions as a transcriptional inhibitor. Dev Biol 249(1):174–190 [PubMed: 12217327]
13. Oshima A, Tanabe H, Yan T, Lowe GN, Glackin CA, Kudo A (2002) A novel mechanism for the regulation of osteoblast differentiation: transcription of periostin, a member of the fasciclin I family, is regulated by the bHLH transcription factor, twist. J Cell Biochem 86(4):792–804 [PubMed: 12210745]
14. el Ghouzzi V, Le Merrer M, Perrin-Schmitt F et al. (1997) Mutations of the TWIST gene in the Saethre-Chotzen syndrome. Nat Genet 15(1):42–46 [PubMed: 8988167]
15. El Ghouzzi V, Legeai-Mallet L, Benoist-Lasselin C et al. (2001) Mutations in the basic domain and the loop-helix II junction of TWIST abolish DNA binding in Saethre-Chotzen syndrome. FEBS Lett 492(1–2):112–118 [PubMed: 11248247]
16. El Ghouzzi V, Legeai-Mallet L, Aresta S et al. (2000) Saethre-Chotzen mutations cause TWIST protein degradation or impaired nuclear location. Hum Mol Genet 9(5):813–819 [PubMed: 10749989]
17. Sosic D, Richardson JA, Yu K, Ornitz DM, Olson EN (2003) Twist regulates cytokine gene expression through a negative feedback loop that represses NF-kappaB activity. Cell 112(2):169–180 [PubMed: 12553906]
18. Stasinopoulos IA, Mironchik Y, Raman A, Wildes F, Winnard P Jr, Raman V (2005) HOXA5-twist interaction alters p53 homeostasis in breast cancer cells. J Biol Chem 280(3):2294–2299 [PubMed: 15545268]
19. Maestro R, Dei Tos AP, Hamamori Y et al. (1999) Twist is a potential oncogene that inhibits apoptosis. Genes Dev 13(17):2207–2217 [PubMed: 10485844]
20. Mironchik Y, Winnard PT Jr, Vesuna F et al. (2005) Twist overexpression induces *in vivo* angiogenesis and correlates with chromosomal instability in breast cancer. Cancer Res 65(23):10801–10809 [PubMed: 16322226]
21. Yang J, Mani SA, Donaher JL et al. (2004) Twist, a master regulator of morphogenesis, plays an essential role in tumor metastasis. Cell 117(7):927–939 [PubMed: 15210113]
22. Wang X, Ling MT, Guan XY et al. (2004) Identification of a novel function of TWIST, a bHLH protein, in the development of acquired taxol resistance in human cancer cells. Oncogene 23(2):474–482 [PubMed: 14724576]
23. Hamamori Y, Sartorelli V, Ogryzko V et al. (1999) Regulation of histone acetyltransferases p300 and PCAF by the bHLH protein twist and adenoviral oncoprotein E1A. Cell 96(3):405–413 [PubMed: 10025406]
24. Vesuna F, Lisok A, van Diest P, Raman V (2021) Twist activates miR-22 to suppress estrogen receptor alpha in breast cancer. Mol Cell Biochem 476(6):2295–2306 [PubMed: 33582945]
25. Vesuna F, Winnard P Jr, Glackin C, Raman V (2006) Twist overexpression promotes chromosomal instability in the breast cancer cell line MCF-7. Cancer Genet Cytogenet 167(2):189–191 [PubMed: 16737925]
26. Vesuna F, van Diest P, Chen JH, Raman V (2008) Twist is a transcriptional repressor of E-cadherin gene expression in breast cancer. Biochem Biophys Res Commun 367(2):235–241 [PubMed: 18062917]
27. Vesuna F, Lisok A, Kimble B, Raman V (2009) Twist modulates breast cancer stem cells by transcriptional regulation of CD24 expression. Neoplasia 11(12):1318–1328 [PubMed: 20019840]
28. Vesuna F, Lisok A, Kimble B et al. (2012) Twist contributes to hormone resistance in breast cancer by downregulating estrogen receptor-alpha. Oncogene 31(27):3223–3234 [PubMed: 22056872]

29. Vesuna F, Bergman Y, Raman V (2017) Genomic pathways modulated by Twist in breast cancer. BMC Cancer 17(1):52 [PubMed: 28086829]
30. Ackerstaff E, Glunde K, Bhujwalla ZM (2003) Choline phospholipid metabolism: a target in cancer cells? J Cell Biochem 90(3):525–533 [PubMed: 14523987]
31. Glunde K, Raman V, Mori N, Bhujwalla ZM (2005) RNA interference-mediated choline kinase suppression in breast cancer cells induces differentiation and reduces proliferation. Cancer Res 65(23):11034–11043 [PubMed: 16322253]
32. Glunde K, Bhujwalla ZM (2007) Choline kinase alpha in cancer prognosis and treatment. Lancet Oncol 8(10):855–857 [PubMed: 17913651]
33. Bhujwalla ZM, Artemov D, Natarajan K, Solaiyappan M, Kollars P, Kristjansen PE (2003) Reduction of vascular and permeable regions in solid tumors detected by macromolecular contrast magnetic resonance imaging after treatment with antiangiogenic agent TNP-470. Clin Cancer Res 9(1):355–362 [PubMed: 12538488]
34. Ogan MD (1988) Albumin labeled with Gd-DTPA: an intravascular contrast-enhancing agent for magnetic resonance blood pool imaging: preparation and characterization. Invest Radiol 23(12):961 [PubMed: 3204001]
35. Tkac I, Starcuk Z, Choi IY, Gruetter R (1999) 1H NMR spectroscopy of rat brain at 1 ms echo time. Magn Reson Med 41(4):649–656 [PubMed: 10332839]
36. Bolan PJ, Meisamy S, Baker EH et al. (2003) In vivo quantification of choline compounds in the breast with 1H MR spectroscopy. Magn Reson Med 50(6):1134–1143 [PubMed: 14648561]
37. Cerami E, Gao J, Dogrusoz U et al. (2012) The cBio cancer genomics portal: an open platform for exploring multidimensional cancer genomics data. Cancer Discov 2(5):401–404 [PubMed: 22588877]
38. Gao J, Aksoy BA, Dogrusoz U et al. (2013) Integrative analysis of complex cancer genomics and clinical profiles using the cBioPortal. Sci Signal. 10.1126/scisignal.2004088
39. Li B, Dewey CN (2011) RSEM: accurate transcript quantification from RNA-Seq data with or without a reference genome. BMC Bioinform 12:323
40. Rouillard AD, Gundersen GW, Fernandez NF et al. (2016) The harmonizome: a collection of processed datasets gathered to serve and mine knowledge about genes and proteins. Database (Oxford). 2016:baw100. 10.1093/database/baw100
41. Mori N, Wildes F, Takagi T, Glunde K, Bhujwalla ZM (2016) The tumor microenvironment modulates choline and lipid metabolism. Front Oncol 6:262 [PubMed: 28066718]
42. Chen F, Zhuang X, Lin L et al. (2015) New horizons in tumor microenvironment biology: challenges and opportunities. BMC Med 13:45 [PubMed: 25857315]
43. Duval K, Grover H, Han LH et al. (2017) Modeling physiological events in 2D vs. 3D cell culture. Physiology (Bethesda). 32(4):266–277 [PubMed: 28615311]
44. Langhans SA (2018) Three-dimensional in vitro cell culture models in drug discovery and drug repositioning. Front Pharmacol 9:6 [PubMed: 29410625]
45. Eckert MA, Lwin TM, Chang AT et al. (2011) Twist1-induced invadopodia formation promotes tumor metastasis. Cancer Cell 19(3):372–386 [PubMed: 21397860]
46. Low-Marchelli JM, Ardi VC, Vizcarra EA, van Rooijen N, Quigley JP, Yang J (2013) Twist1 induces CCL2 and recruits macrophages to promote angiogenesis. Cancer Res 73(2):662–671 [PubMed: 23329645]
47. Liu A, Huang C, Cai X, Xu J, Yang D (2016) Twist promotes angiogenesis in pancreatic cancer by targeting miR-497/VEGFA axis. Oncotarget 7(18):25801–25814 [PubMed: 27015364]
48. Krishnamachary B, Glunde K, Wildes F et al. (2009) Noninvasive detection of lentiviral-mediated choline kinase targeting in a human breast cancer xenograft. Cancer Res 69(8):3464–3471 [PubMed: 19336572]
49. Mori N, Glunde K, Takagi T, Raman V, Bhujwalla ZM (2007) Choline kinase down-regulation increases the effect of 5-fluorouracil in breast cancer cells. Cancer Res 67(23):11284–11290 [PubMed: 18056454]
50. Bansal A, Harris RA, DeGrado TR (2012) Choline phosphorylation and regulation of transcription of choline kinase alpha in hypoxia. J Lipid Res 53(1):149–157 [PubMed: 22025560]

51. Semenza GL (2003) Targeting HIF-1 for cancer therapy. Nat Rev Cancer 3(10):721–732 [PubMed: 13130303]

52. Yang MH, Wu MZ, Chiou SH et al. (2008) Direct regulation of TWIST by HIF-1alpha promotes metastasis. Nat Cell Biol 10(3):295–305 [PubMed: 18297062]

53. Russell S, Xu L, Kam Y et al. (2022) Proton export upregulates aerobic glycolysis. BMC Biol 20(1):163 [PubMed: 35840963]

54. Albergaria A, Paredes J, Sousa B et al. (2009) Expression of FOXA1 and GATA-3 in breast cancer: the prognostic significance in hormone receptor-negative tumours. Breast Cancer Res 11(3):R40 [PubMed: 19549328]

55. Xu Y, Qin L, Sun T et al. (2017) Twist1 promotes breast cancer invasion and metastasis by silencing Foxa1 expression. Oncogene 36(8):1157–1166 [PubMed: 27524420]

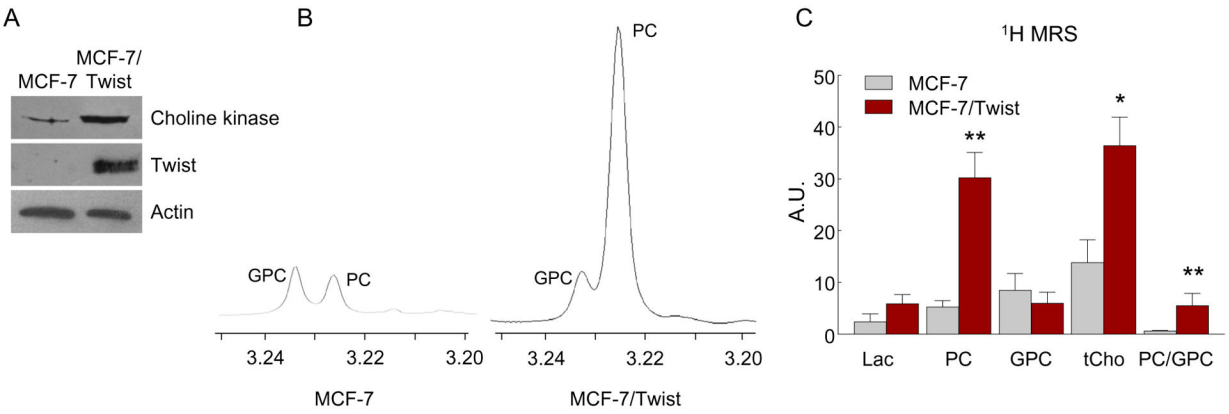

Fig. 1.

CKA expression and NMR spectra of MCF-7 and MCF-7/Twist cells. **A** Immunoblot showing increased choline kinase expression in MCF-7/Twist cells. **B** ^{1}H MR spectra of MCF-7 wild type cells and MCF-7/Twist overexpressing cells. Spectral regions from the glycerophosphocholine (GPC) and phosphocholine (PC) regions are displayed. Spectra were obtained from comparable cell numbers. **C.** Histogram displaying levels of various metabolites as well as tCho and PC/GPC ratio in MCF-7 and MCF-7/Twist cells

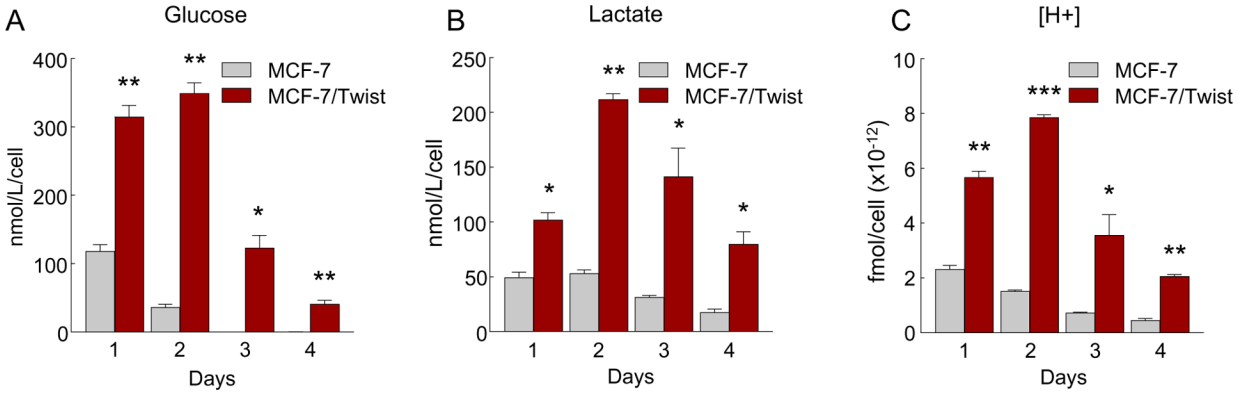

Fig. 2.

Glucose, Lactate, and [H +] levels in extracellular spent media. **A** Histogram displaying changes in extracellular glucose levels in MCF-7 and MCF-7/Twist cells over a four-day period. **B** Graph displaying the changes in extracellular lactate in MCF-7 and MCF-7/Twist cells. **C** Histogram displaying increased [H +] in MCF-7/Twist cells compared to MCF-7 cells

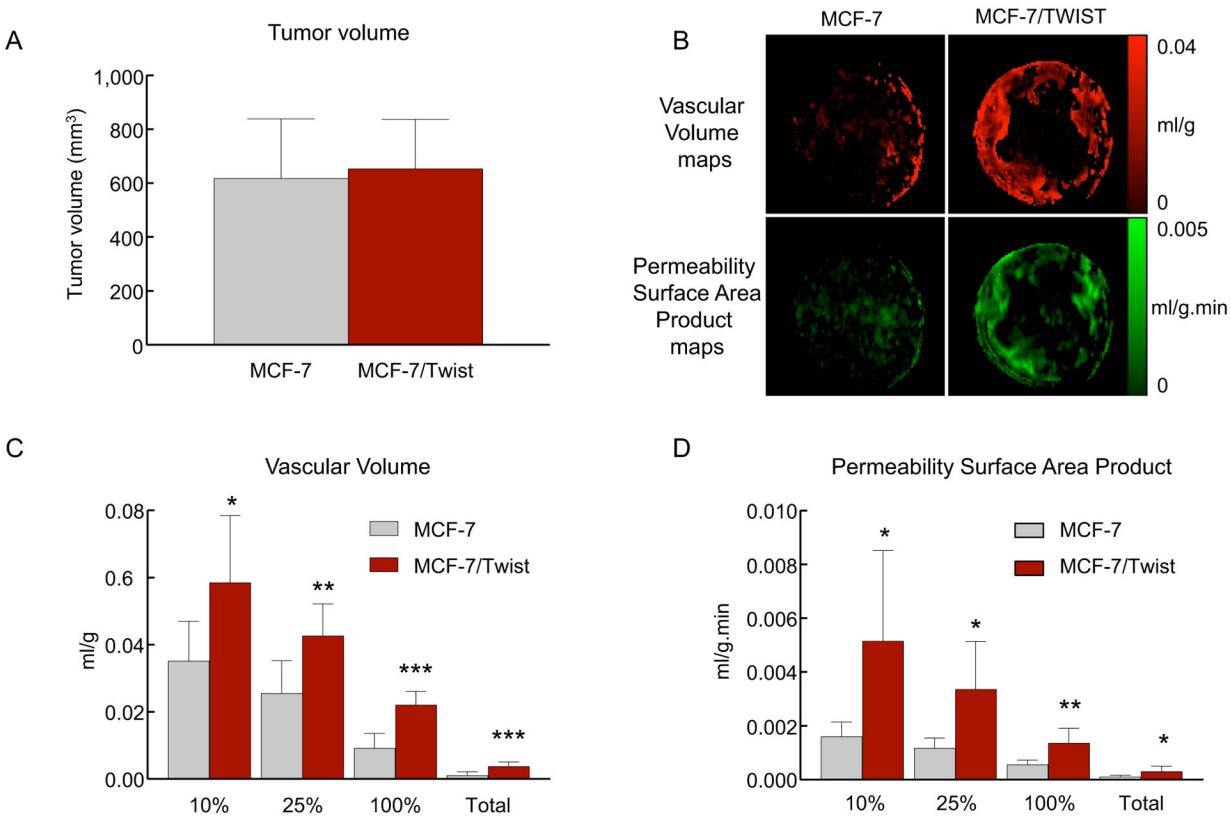

Fig. 3.

Magnetic resonance images of MCF-7 and MCF-7/Twist xenografts in SCID mice. **A** Volume of MCF-7 and MCF-7/Twist tumors at analysis. **B** Representative 3D volume rendering of vascular volume (red) and permeability surface area product (green) of the tumors obtained with in vivo dynamic MRI. **C** Histogram of vascular volume in MCF-7 and MCF-7/Twist xenografted tumors (pooled data for 5 animals in each group). **D** Histogram of the vascular permeability in MCF-7 and MCF-7/Twist xenografted tumors (pooled data for 5 animals in each group). Highest 10%, 25%, and 100% of all non-zero values, and total values are shown. (Mean ± SD, $n = 4$)

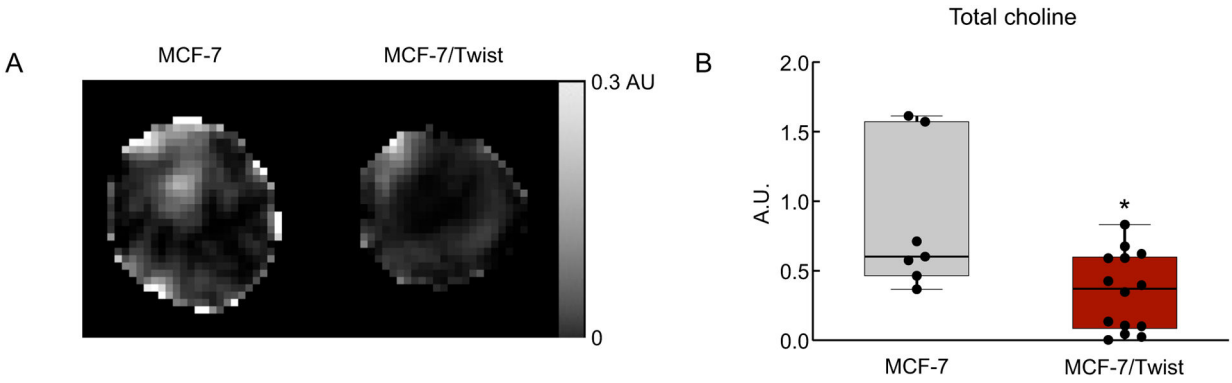

Fig. 4.

Metabolic maps of total choline levels. **A** Total choline maps of MCF-7 tumor and MCF-7/Twist tumor acquired on a 9.4 T spectrometer (TE = 272 ms, TR = 1000 ms, NA = 8). **B** Box and whiskers plots of total choline concentrations of MCF-7 ($n = 7$) and MCF-7/Twist ($n = 14$) tumors

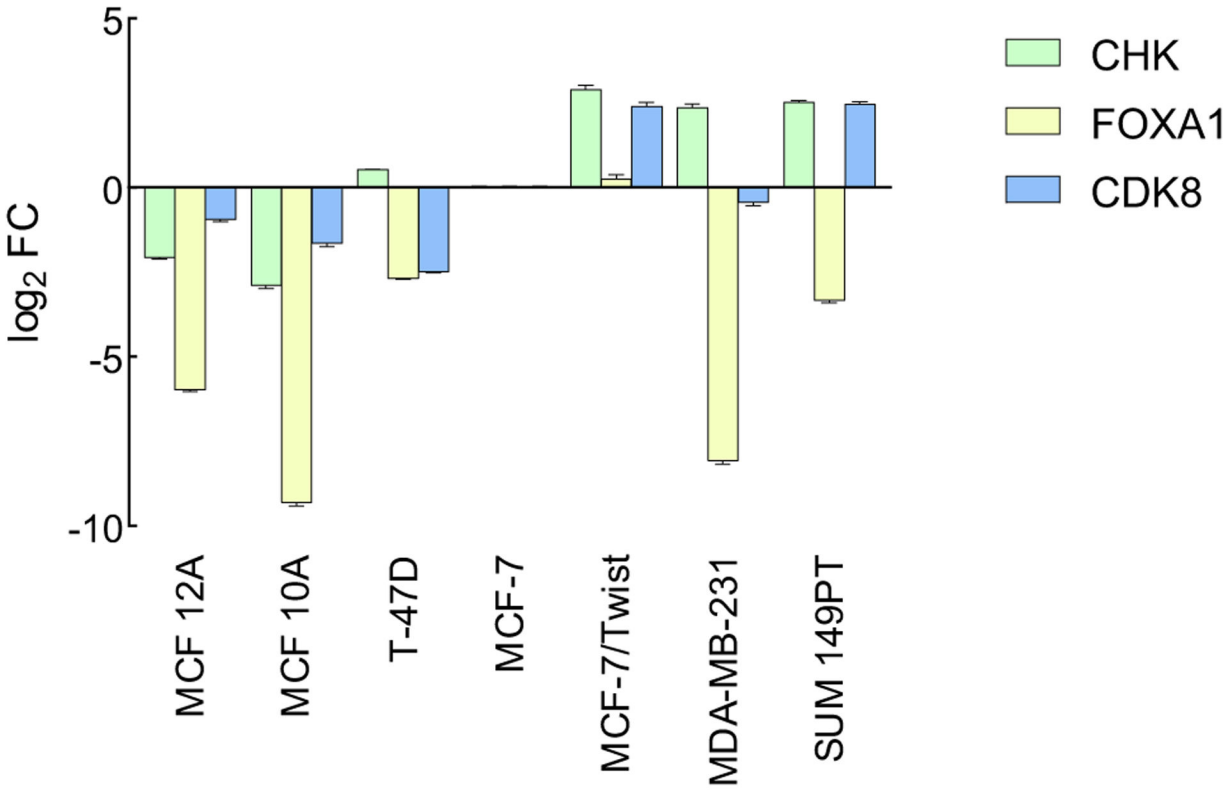

Fig. 5.

RT-qPCR of CHKA, FOXA1, and CDK8. RT-qPCR of CHKA, FOXA1, and CDK8 genes in normal cell lines (MCF 12A, MCF 10A), ER positive cell lines (T-47D, MCF-7), and ER-negative cell lines (MCF-7/Twist, MDA-MB-231, SUM-149PT). Expression values are indicated as log2 fold-change

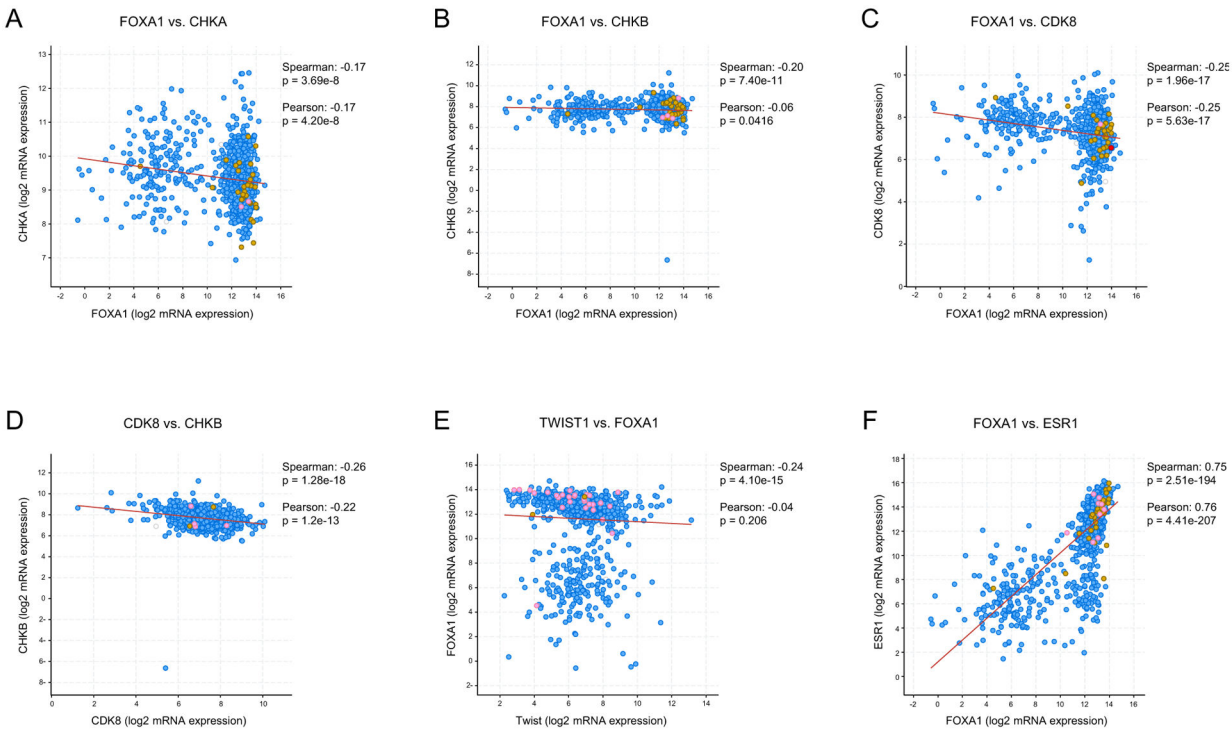

Fig. 6.

Analysis of gene expression from TCGA breast tumor database. **A** Correlation plot of FOXA1 vs. CHKA mRNA expression. **B** Correlation plot of FOXA1 vs. CHKB mRNA expression. **C** Correlation between FOXA1 and CDK8. **D** Correlation plot between CDK8 and CHKB mRNA expression. **E** Correlation plot between Twist and FOXA1 mRNA expression. **F** Representation of the regulation of CHKA and CHKB by Twist via FOXA1 and CDK8. Black arrows indicate data in this manuscript. Yellow lines indicate TCGA and ENCODE data. Lines indicate upregulation while dashed lines indicate repression

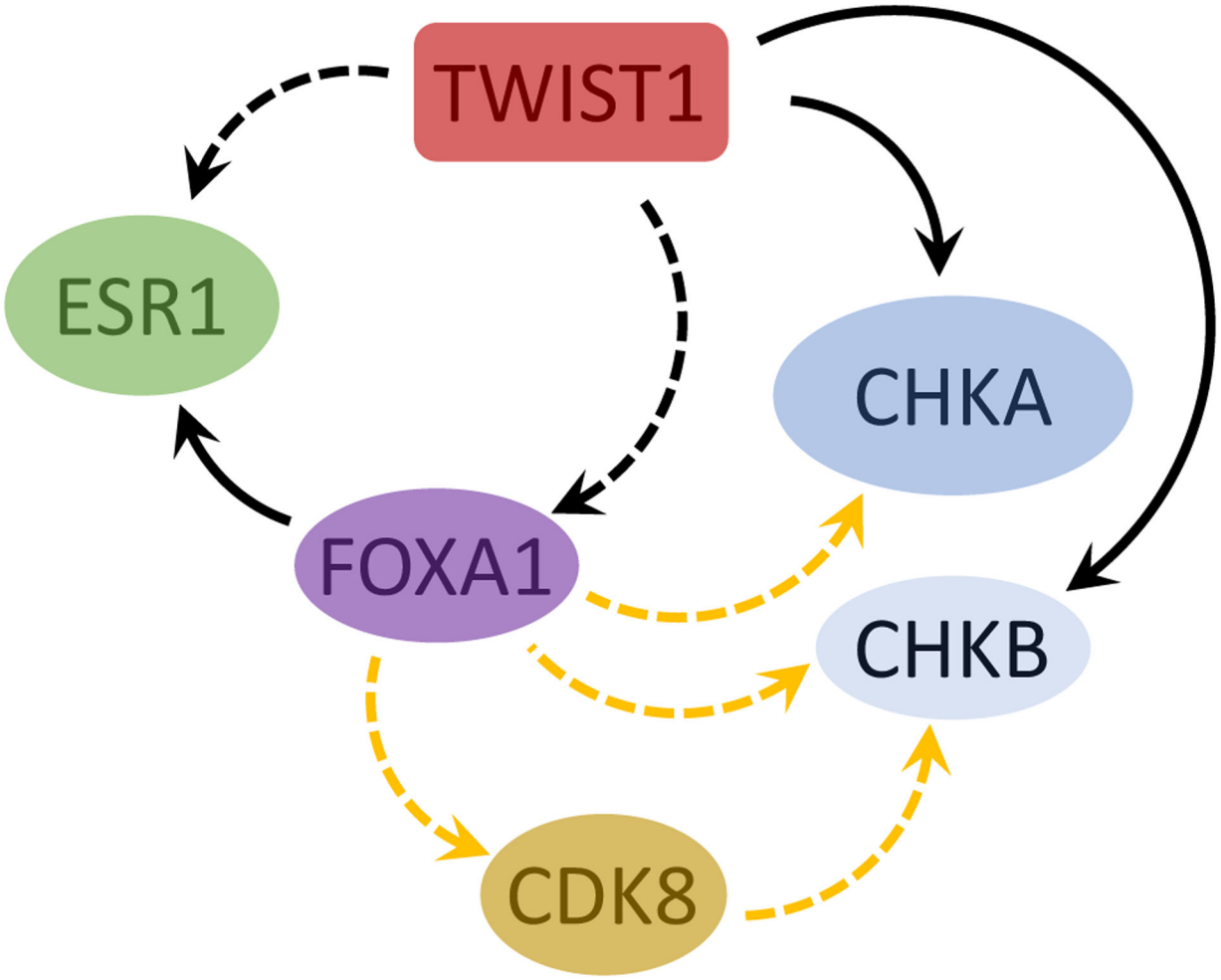

Fig. 7.

Representation of Twist driven pathways regulating choline kinase. Twist regulated CHKA and CHKB directly as well as indirectly through FOXA1 and CDK8. Solid arrows depict upregulation while dashed arrows indicate inhibition. Black arrows indicate data from this manuscript and ENCODE while yellow arrows indicate ENCODE data